Anal. Chem. **2006,** *78,* 2905−2917

Accelerated Articles

Structural Identification of Highly Polar Nontarget Contaminants in Drinking Water by ESI-FAIMS-Q-TOF-MS

Jassim Sultan and Wojciech Gabryelski*

Department of Chemistry, University of Guelph, Guelph, Ontario, N1G 2W1, Canada

Drinking water is a complex mixture that contains thousands of naturally occurring and anthropogenic contaminants. Liquid chromatography−mass spectrometry (LC−MS) methods have gained a tremendous popularity in monitoring nonvolatile, highly polar, and thermally labile components in drinking water. It is well recognized, however, that there are difficulties or limitations of LC−MS methods associated with (1) significant resources (time and effort) involved in sample preparation (preconcentration, fractionation, separation), (2) low screening capacity for target contaminants, and (3) insufficient capabilities for structural identification (elucidation) of nontarget contaminants. Consequently, LC−MS methods are mainly used for the detection of target contaminants (compounds identified in drinking water before), seldom for the structural identification of abundant nontarget pollutants (unidentified pollutants in drinking water), and almost never for the structural identification of nontarget components at a trace level. The paper presents a new method of electrospray ionization high field asymmetric waveform ion mobility spectrometry mass spectrometry (ESI-FAIMS−MS), which can detect a large number of water pollutants in a quick and convenient fashion without preconcentration, fractionation, derivatization, or column separation. Most importantly, the method provides structural identification of nontarget contaminants including species present in drinking water at a sub-parts-per-billion concentration level. The identification of previously unknown contaminants was based on mass measurements of investigated ions and their fragments in mass and tandem mass spectrometry. Elemental compositions of these ions, determined by mass measurements, were used to link dissociation patterns of investigated species with their chemical structures. Characterization of nontarget contaminants of chlorine-treated drinking water by ESI-FAIMS−MS has revealed many previously unknown disinfection byproducts. The most intriguing compound, from a group of highly polar hydroxycarboxylic acids discovered in the study, was the most abundant component of drinking water, glycolic acid. Glycolic acid (toxic to kidneys and associated with a moderate maternal toxicity) has never been considered as a drinking water contaminant, despite the fact that it is present in drinking water at a higher concentration (high ppm) than concentrations of highly polar water pollutants that had attracted most attention in the past. The process of structural elucidation of discovered pollutants, including ultratrace contaminants representing a variety of carboxylic acids, will be presented in detail. The structural identification of highly polar contaminants in drinking water presented in the paper is rarely reported in the literature. The key experimental feature of the ESI-FAIMS−MS method is FAIMS separation, which significantly improves the identification capabilities of mass spectrometry.

Drinking water is a complex mixture containing thousands of naturally occurring and anthropogenic contaminants that are a primary concern to ensure its safety. A number of recently identified pollutants[1] associated with health risks has increased significantly with the development of analytical methods[2] capable of monitoring the quality of water with respect to a variety of compounds including chemical species present at very low but still relevant concentrations. Gas chromatography−mass spectrometry (GC/MS) methods have greatly contributed to the characterization of

* To whom correspondence should be addressed. Tel: 519-824-4120 ext. 53850. Fax: 519-766-1499. E-mail: wgabryel@uoguelph.ca.

(1) Richardson, S. D. Drinking Water Disinfection By-Products. In *Encyclopedia of Environmental Analysis and Remediation*; R. A. Meyers, Ed.; John Wiley & Sons: New York, 1998; Vol. 3, p 1398.
(2) Richardson, S. D. *Anal. Chem.* **2005**, *77*, 3807.

10.1021/ac060384x CCC: $33.50
Published on Web 04/05/2006

volatile[3] and semivolatile[4] contaminants in water whereas liquid chromatography−mass spectrometry (LC−MS) methods[5−7] have been utilized to extend the investigation of water pollution to nonvolatile, highly polar, and thermally labile compounds of pharmaceuticals, pesticides, steroids, and personal care products. Despite well-established analytical methodology, current assessments of the quality of drinking water, with respect to highly polar contaminants, are far from definitive due to the lack of screening capacity for a wide range of already known pollutants and sufficient identification capabilities for unknown and potentially hazardous components of drinking water.

Significant time and effort are required for sample preparation in trace analysis of water pollutants by LC−MS. A preconcentration of sample's components by factors of 100−100 000 is necessary to improve their detection, which is compromised by chemical noise associated with sample matrix. Liquid chromatography−tandem mass spectrometry (LC−MS/MS) methods,[8−10] in which multiple mass-resolving devices (e.g., triple-quadrupole) are used to eliminate the chemical background, provide improved detection capabilities and alleviate requirements for sample preparation (preconcentration). These methods, however, have a limited screening capacity because each LC−MS/MS procedure can only be used for the detection of a small group of preselected compounds (target analytes), usually not more than 30 at a time. The retention behavior of target compounds during separation and their specific fragmentation in tandem mass spectrometry must be known or determined by using available chemical standards. Consequently, although the combination of liquid chromatographic separation with triple-quadrupole MS/MS detection offers advantages in terms of selectivity, it is of limited use for the identification of nontarget analytes.

The identification of nontarget contaminants could be accomplished by using spectral databases (comparative identification approach) or molecular weight and MS/MS information from accurate mass determinations (de novo identification approach). The compound identification based on spectral databases is more feasible with GC/MS, which can rely on well over 100 000 electron ionization spectra of thermally stable compounds. LC−MS/MS databases are usually user created because spectral data obtained from soft ionization techniques combined with MS/MS are highly dependent upon instrument design and operating parameters. Similar data for LC−MS/MS[11] are restricted to a few hundred compounds. De novo identification methods rely on mass spectrometers capable of providing high resolution and high accuracy of mass measurements in MS and MS/MS. The elucidation of elemental compositions and chemical structures of nontarget species could be accomplished based on spectral data acquired by many types of mass analyzers. LC−MS/MS methods, utilizing high-performance mass spectrometry in water analysis, however, are mainly used for the detection of target contaminants, seldom for the structural identification of most abundant nontarget pollutants, and almost never for the structural identification of nontarget pollutants at trace level.[12] The difficult process of structural elucidation of nontarget contaminants in water by LC−MS/MS is rather problematic because the quality of spectral information is compromised by interferences from liquid mobile phase and complex sample matrix.

The introduction of electrospray ionization high field asymmetric waveform ion mobility spectrometry mass spectrometry (ESI-FAIMS−MS) has addressed some tangible needs in water analysis. The key experimental feature of the FAIMS method is the capability for gas-phase ion separation prior to mass spectrometry analysis. The FAIMS-MS method[13] significantly reduces the background of interfering species from liquid sample matrix and selectively detects, in a matter of few minutes, positive and negative ions of trace analytes of interest with no preconcentration, derivatization, or liquid separation. Therefore, a number of rapid, sensitive, and selective protocols have been developed for the analysis of haloxides,[14] toxic microcystins,[15] haloacetic acids,[16] and naphthenic acids[17] in water. The ESI-FAIMS−MS technique has been used in the analysis of target pollutants only, and its potential for the structural identification of nontarget contaminants by tandem mass spectrometry has never been evaluated. This paper demonstrates unique analytical capabilities of ESI-FAIMS with high-performance mass spectrometry for detection and comprehensive characterization of previously unknown contaminants in drinking water.

EXPERIMENTAL SECTION

A diagram of the ESI-FAIMS−MS instrument is shown in Figure 1. Water samples (diluted with methanol (1/10 v/v)) were delivered to the electrospray source at a flow rate of 1 μL/min by using a syringe pump. The electrospray source consisted of a length of fused-silica capillary (FSC) (30 cm × 50 μm i.d. × 180 μm o.d.) that protruded through a stainless steel capillary (2 cm × 200 μm i.d. × 430 μm o.d.). The polyimide coating was removed from the tip of the FSC. The extension of the FSC end from the tip of the metal capillary was adjusted to provide stable ESI operation. The metal capillary was kept at a potential of −3300 V. The tip of the needle was located ~1 cm from the 2-mm opening in the curtain plate of the FAIMS device and positioned at 45° with respect to the plate surface. The curtain plate was electrically insulated from the outer cylinder of the FAIMS device and kept at the potential of −1000 V. The carrier gas (97.5% N_2 and 2.5% CO_2) was purified by charcoal/molecular sieve filters and introduced into the FAIMS analyzer region at a total flow of 2 L/min.

(3) *The Characterization of Volatile Organics in Water, and Effluent by Purge-and-Trap (PT) Gas Chromatography−Mass Spectrometry (GC-MS)*; Ministry of the Environment, Laboratory Services Branch: Etobicoke, ON, Canada, 1999.
(4) *The Characterization of Extractable Organics in Water, Waste, and Soil and Effluent by Gas Chromatography−Mass Spectrometry (GC-MS)*; Ministry of the Environment, Laboratory Services Branch: Etobicoke, ON, Canada, 1999.
(5) Lopez de Alda, M. J.; Barcelo, D. *Fresenius J. Anal. Chem.* **2001**, *371*, 437.
(6) Richardson, S. D. *Anal. Chem.* **2002**, *74*, 2719.
(7) Ternes, T. A. *Trends Anal. Chem.* **2001**, *20*, 419.
(8) Hirsch, R.; Ternes, T. A.; Haberer, K.; Mehlich, A.; Ballwanz, F.; Kratz, K. *J. Chromatogr., A* **1998**, *815*, 213.
(9) Steen, R. J. C. A.; Hogenboom, A. C.; Leonards, P. E. G.; Peerboom, R. A. L.; Cofino, W. P.; Brinkman U. A. Th. *J. Chromatogr., A* **1999**, *857*, 157.
(10) Vanderford, B. J.; Pearson, A. R.; Rexing, D. J.; Snyder, S. A. *Anal. Chem.* **2003**, *75*, 6265.
(11) Kienhuis, P. G. M.; Geerding, R. B. *Trends Anal. Chem.* **2000**, *19* (7), 460.
(12) Zwiener, C.; Richardson, S. D. *Trends Anal. Chem.* **2005**, *24* (7), 613.
(13) Ells, B.; Barnett, D. A.; Froese, K. L.; Purves, R. W.; Hrudey, S.; Guevremont, R. *Anal. Chem.* **1999**, *71*, 4747.
(14) Barnett, D. A.; Guevremont, R.; Purves, R. W. *Appl. Spectrosc.* **1999**, *53*, 1367.
(15) Ells, B.; Froese, K.; Hrudey, S. E.; Purves, R. W.; Guevremont, R.; Barnett, D. A. *Rapid Commun. Mass Spectrom.* **2000**, *14*, 1538.
(16) Gabryelski, W.; Wu, F.; Froese, K. L. *Anal. Chem.* **2003**, *75*, 2478.
(17) Gabryelski, W.; Froese, K. L. *Anal. Chem.* **2003**, *75*, 4612.

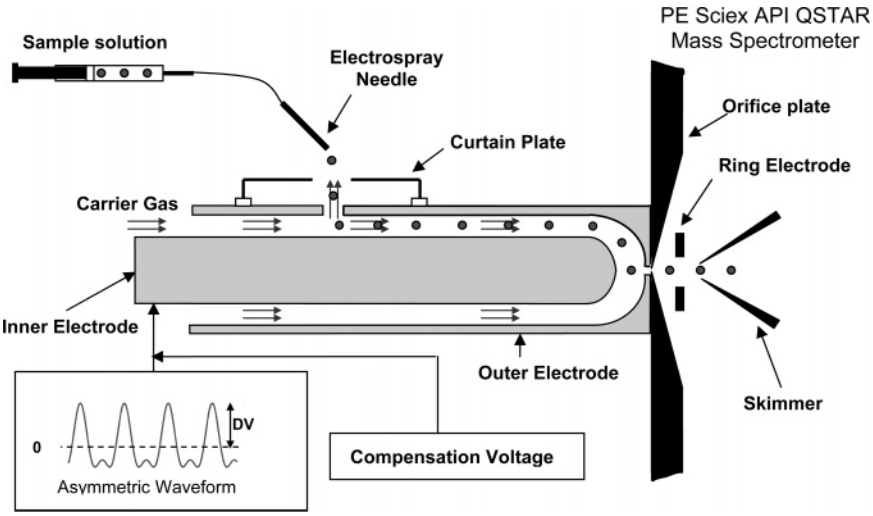

Figure 1. Schematic diagram of the ESI-FAIMS−MS instrument.

The gas was split into two flows with a larger portion of the gas flowing out of the opening in the curtain plate as a countercurrent flow against the arriving electrospray-generated ions and a smaller portion of the total gas flow carried these ions through the FAIMS analyzer region to the entrance of the mass spectrometer. The FAIMS separation device (Figure 1) consisted of two concentric cylinders. The end of the inner cylinder (16-mm o.d.) facing the mass spectrometer was machined to a spherical shape. The inner part of the outer cylinder (20-mm i.d.) facing the mass spectrometer was machined to a concave spherical shape. The spacing between the inner and the outer electrodes in the cylindrical part of the FAIMS analyzer region was 2 mm. The distance between the spherical surfaces of the inner and the outer electrodes was adjusted to 2.32 mm. The surface of the outer cylinder at the mass spectrometer side was flat with a 1-mm aperture in the center. This surface made electrical contact with the orifice plate of the PE Sciex API QStar Pulsar time-of-flight mass spectrometer. An asymmetric waveform,[18] at dispersion voltage −3500 V and frequency of 750 kHz, was applied to the inner cylinder of the FAIMS device along with the dc compensation voltage. The relative amplitude of the sinusoidal wave and its harmonic[19] were ~3:1.

The principles of ion separation in FAIMS has been described in detail elsewhere[20,21] and are only briefly summarized here. To separate two ions in FAIMS, the relative ion mobility, expressed as a ratio of the ion mobility at high electric field and the ion mobility at low electric field, has to be different for these two ions. High and low, electric field conditions are generated between the plates of FAIMS (Figure 1) by application of an asymmetric waveform to the inner electrode. During one cycle of the waveform, an ion experiences a short duration of high electric field and moves at high field mobility toward one of the electrodes. During the same cycle of the waveform, the ion also experiences a longer duration of oppositely directed low electric field and moves with low field ion mobility toward the opposite electrode. The waveform is designed in such a way that if the mobility of the ion is the same under high and low field conditions, the ion does not experience any displacement from the center in the space between two electrodes. The difference in relative ion mobility at high and low field, however, will result in a constant drift of the ion toward one of the cylindrical electrodes. To transport the ion through the FAIMS, a dc compensation voltage (CV) voltage has to be applied to the inner electrode to compensate for the ion drift. The ion is transmitted through FAIMS and sampled by the mass spectrometer only when an appropriate value of the compensation voltage is used. Although FAIMS separation is continuous in nature, the CV can be scanned to obtain the distribution of ions transmitted through FAIMS at different separation conditions.

Following separation, ions were transported from the atmospheric pressure region of FAIMS through the 250-μm-diameter opening in the orifice plate into the low-pressure region of the source equipped with the ring electrode assembly and the skimmer. The Q-TOF instrument was operated either in full scan mode (MS) to pass all the ions through rf-only quadrupole for TOF detection or in product ion mode (MS/MS) so that a product ion spectrum was obtained for each precursor ion. The mass detector provided high speed of detection, tandem mass spectrometry capabilities, high mass resolution, and high accuracy of mass measurement. The internal mass calibration method was implemented for calibration acquired mass spectra with masses of known water pollutants (e.g., HSO_4^-, Cl_3CCOO^-) used as a reference. The Analyst Mass Calculator program was used for determination of elemental compositions.

Drinking water was acquired at one location in a Canadian city. Sampling and preservation of drinking water were carried out according to requirements of the EPA Method 552.2. Aside from dilution with methanol, no sample cleanup, filtering, or preparation was performed. The determination of blank was performed for all species examined in the study. The signal for each investigated contaminant from the water sample was at least 10 times higher than the corresponding signal originating from the blank. HPLC-grade methanol and ammonium chloride were purchased from Fisher Scientific Co. (Nepean, ON, Canada). Trichloroacetic acid

(18) Guevremont, R.; Barnett, D. A.; Purves, R. W.; Vandermey, J. *Anal. Chem.* **2000**, *72*, 4577.
(19) Viehland, L. A.; Guevremont, R.; Purves, R. W.; Barnett, D. A. *Int. J. Mass Spectrom.* **2000**, *197*, 123.
(20) Buryakov, I.; Krylov, E.; Nazarov, E.; Rasulev, U. *Int. J. Mass Spectrom. Ion Processes* **1993**, *128*, 143.
(21) Purves, R. W.; Guevremont, R. *Anal. Chem.* **1999**, *71*, 2346.

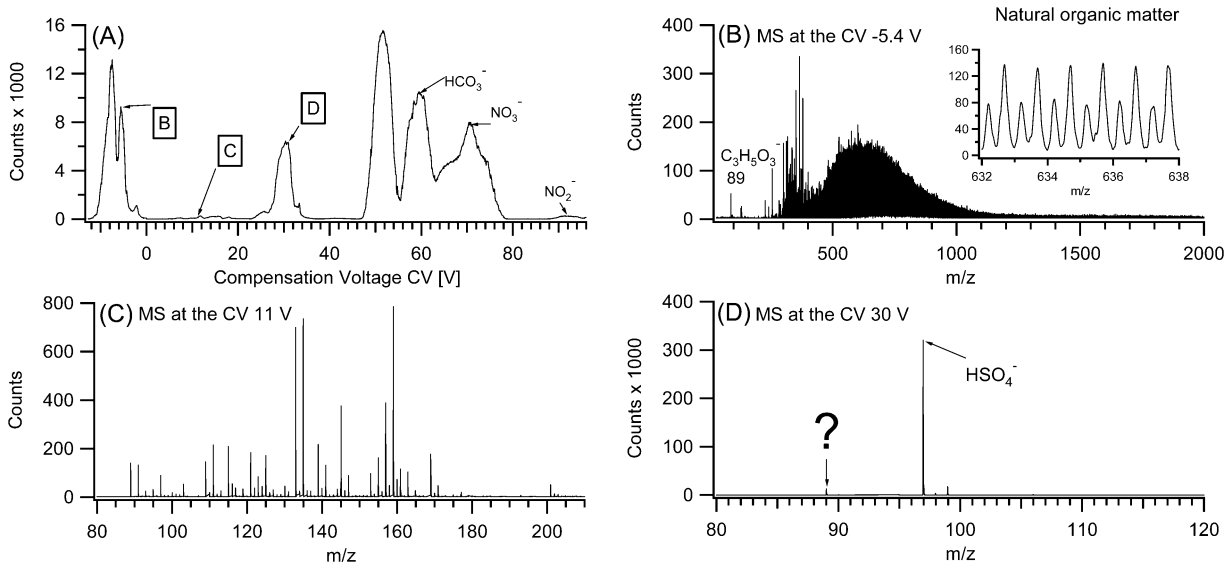

Figure 2. Detection of contaminants in drinking water by ESI-FAIMS−MS. (A) TICV spectrum, (B) mass spectrum at CV −5.4 V (500 scans), (C) mass spectrum at CV 11.0 V (500 scans), (D) mass spectrum at CV 30 V (50 scans).

(TCA), D-lactic acid, L-lactic acid, L-tryptophan, and glycolic acid were supplied by Supelco (Oakville, ON, Canada).

RESULTS AND DISCUSSION

Figure 2 shows spectra acquired in the ESI-FAIMS−MS analysis of tap water. A 10-fold dilution of drinking water with methanol[16] was the only sample preparation step prior to the analysis. The methanol-diluted sample was analyzed directly in the negative mode of electrospray without preconcentration, fractionation, derivatization, or column separation. Ionized sample components were separated by FAIMS and detected by Q-TOF MS. Figure 2A shows the total ion compensation voltage (TICV) spectrum acquired by scanning the CV from −14 to 96 V (with a 0.1-V interval) and detecting (for 1 s) the total intensity of ions transmitted through FAIMS at each CV separation step. The TICV spectrum is similar to a total ion chromatogram in LC−MS. The CV distribution of detected species, however, is not based on principles of chromatographic separation but rather on high and low electric field mobilities of observed gas-phase ions. A CV scanning rate (0.1 V/s in Figure 2A) can be increased or decreased to control separation time in FAIMS (~20 min in Figure 2A) in a similar way to controlling elution times in LC by changing solvent strength. The most important operational difference between FAIMS and LC separation is that the CV scan can be stopped at any time and any CV for a long period of time. Panels B−D in Figure 2 show mass spectra acquired by stopping (parking) the CV scan at three different CV settings and detecting ions transmitted through FAIMS at these conditions for an extended period of time. The mass spectrum in Figure 2B represents a sum of 500 spectral TOF scans (acquisition time of 500 s) and demonstrates the direct detection of negatively charged ions of components natural organic matter (NOM) separated at the CV −5.4 V. The mass spectrum (Figure 2C) represents ions of ultratrace components of drinking water separated at the CV 11 V. Figure 2D shows the mass spectrum of species detected in water at the CV 30 V. Mass spectra (not shown), acquired in the entire CV separation range (−14 to 94 V), showed thousands of ions detected in the full scan mode by Q-TOF following FAIMS separation. A high screening capacity observed for the method led to an important issue related to the identification of detected unknown species. An identification method based on matching masses and separation CVs of ions of chemical standards with those of the ions detected in the sample will recognize these target contaminants, but a large number of detected ions, representing even the most abundant components of drinking water, will still remain unknown. The advantage of de novo identification approach, presented in this paper, is that one might determine chemical identity of species actually observed in the sample. The identification of several detected ions was straightforward. For example, the mass measurement and resulting elemental composition of the m/z 97 ion detected at the CV 30 V (Figure 2D), together with the characteristic pattern of isotopic peaks at m/z 97, 98, and 99, allowed for the recognition of HSO_4^-. Mass measurements of other small ions provided identification of NO_2^-, NO_3^-, and HCO_3^-. These inorganic anions are separated in FAIMS at high CVs (Figure 2A).

The mass spectrum in Figure 2D shows that, in addition to HSO_4^-, another ion at m/z 89 was separated and detected at the CV 30 V. The identification process of the m/z 89 ion was initiated by examining the selected ion CV (SICV) spectrum of m/z 89 ions (Figure 3). The SICV spectrum shows the CV distribution of ions with the same nominal m/z of 89, and it is similar to a typical selected ion chromatogram (LC−MS). Three m/z 89 peaks, observed in the SICV spectrum of m/z 89 at CVs −5.4, 30.4, and 33.8 V (Figure 3B), indicate that three structurally different m/z 89 ions were detected in the sample. The determination of elemental compositions of these ions was accomplished by mass measurements. Table 1 lists measured masses of m/z 89 ions detected at different CVs as well as masses (calculated) and elemental compositions of singly charged negative ions in a ±100 ppm mass range relative to the measured masses of investigated ions. The results of mass measurements show that three m/z 89 ions have the same elemental composition $C_3H_5O_3^-$.

One can find at least nine $C_3H_6O_3$ structural isomers that would form corresponding $C_3H_5O_3^-$ ions in the negative mode of

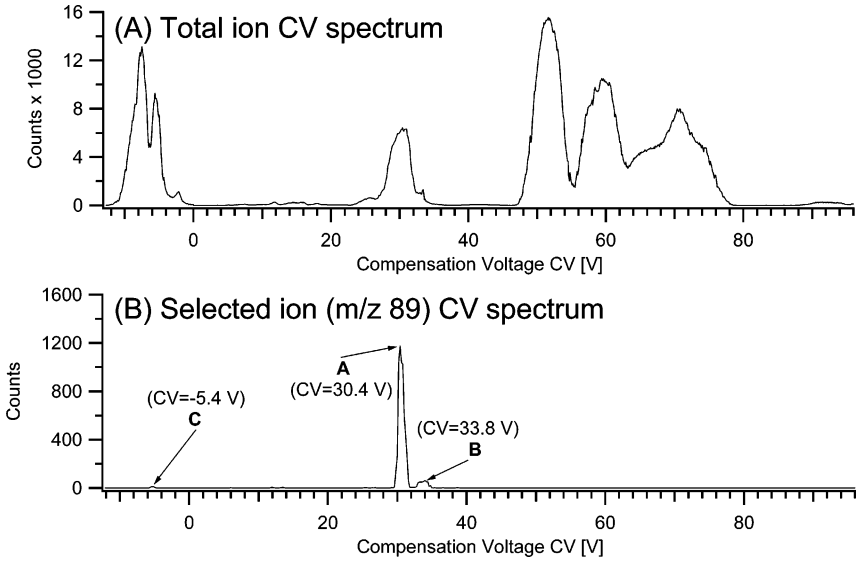

Figure 3. FAIMS separation of unidentified contaminants of drinking water at *m*/*z* 89. (A) TICV spectrum of water sample and (B) SICV spectrum of *m*/*z* 89 ions.

Table 1. Determination of Elemental Composition of *m*/*z* 89 Ions Detected in Drinking Water

negative ions		error (ppm)		
elemental compn	calcd *m*/*z* (amu)	CV 30.4 V (A) 89.0245	CV 33.8 V (B) 89.0239	CV −5.4 V (C) 89.0251
$C_3H_5O_3$	89.0244	1.1	−5.6	6.7
$CH_3N_3O_2$	89.0230	16.8	10.1	23.6
$C_2H_5NNa_2$	89.0222	25.8	19.1	32.6
C_6H_3N	89.0270	−28.1	−34.8	−21.3
$C_2H_6N_2P$	89.0274	−32.6	−39.3	−25.8
C_3H_7NS	89.0304	−66.2	−73.1	−59.5
$C_2H_5N_2S_2$	89.0178	75.3	68.5	82.0
C_4H_6Cl	89.0163	92.1	85.4	98.9
C_3H_6PO	89.0161	94.4	87.6	101
CH_4N_3P	89.0148	109	102	116

electrospray. The chemical identity of even small organic anions such as $C_3H_5O_3^-$ has to be investigated in tandem mass spectrometry. MS/MS data for the $C_3H_5O_3^-$ ion separated by FAIMS at the CV 30.4 V are shown in Figure 4A and MS/MS data for the $C_3H_5O_3^-$ ion separated by FAIMS at the CV 33.8 V are presented in Figure 4B. Mass measurements of fragment ions generated from respective $C_3H_5O_3^-$ precursors allowed for the confident assignment of their elemental compositions (accuracy of mass measurement (ppm) of all identified fragment ions is given in Figure 4). The elemental composition of molecular and fragment ions was used to establish fragmentation patterns of $C_3H_5O_3^-$ isomers. The final and most difficult step of structural elucidation was based on examining feasible chemical structures of $C_3H_5O_3^-$ ions, which would be consistent with information obtained from tandem mass spectrometry. The process of structural elucidation of $C_3H_5O_3^-$ isomers is illustrated in Figure 5 where chemical structures of molecular ions and their fragments have been established based on fragmentation patterns observed in tandem mass spectrometry.

The $C_3H_5O_3^-$ ion detected at the CV 30.4 V (Figure 4A) was identified as 2-hydroxypropanoate, the product of electrospray ionization of 2-hydroxypropanoic acid. Figure 5A shows fragmentation patterns of 2-hydroxypropanoate leading to the formation of diagnostic fragments at *m*/*z* 87, 71, 45, and 43. The postulated dissociation of 2-hydroxypropanoate (structure in the box) is initiated by redistribution of negative charge leading to the proton transfer (PT) from the hydroxyl to the carboxyl group and formation of anion with negative charge localized at α-oxygen. This anion dissociates through a three-member-ring intermediate complex in which charge redistribution leads to elimination of H_2O and formation of resonance-stabilized ketene-like ion at *m*/*z* 71. The alternative process of elimination of H_2, followed by PT, generates the *m*/*z* 87 ion. Rearrangement of the ion produced by H_2 loss and subsequent proton transfer leads to formation of the *m*/*z* 43 ion and the *m*/*z* 45 ion as a result of elimination of CO_2 and H_2CCO (ketene), respectively. It is important to note that 2-hydroxypropanoate does not dissociate by direct elimination of CO_2. The dissociation product of this particular reaction, with elemental composition of C_2H_5O, was not observed in the MS/MS spectrum of 2-hydroxypropanoate. The $C_3H_5O_3^-$ ion detected at CV 33.8 V (Figure 4B) was identified as 3-hydroxypropanoate. Figure 5B shows proposed fragmentation patterns of 3-hydroxypropanoate leading to the formation of diagnostic products at *m*/*z* 87, 71, 61, 59, 45, and 43. The dissociation of 3-hydroxypropanoate (structure in the box) is initiated by charge redistribution leading to PT from the hydroxyl to the carboxyl group with formation of the anion with charge localized at β-oxygen. This ion dissociates through a four-member-ring intermediate complex by elimination of C_2H_4 and H_2O to form the *m*/*z* 61 ion and the *m*/*z* 71 ion, respectively. An alternative process of the elimination of H_2 generates the *m*/*z* 87 ion which, after PT, produces the *m*/*z* 45 ion and the *m*/*z* 43 ion by loss of H_2CCO (ketene) and CO_2, respectively. The *m*/*z* 59 ion results from elimination of CH_2O from the molecular ion of 3-hydroxypropanoate with charge localized at β-oxygen. 3-Hydroxypropanoate does not dissociate by direct elimination of CO_2. The dissociation product of this particular reaction with elemental composition of C_2H_5O was not observed in the MS/MS spectrum of 3-hydroxypropanoate. The fragmentation of 2- and 3-hydroxypropanoate (and all other species

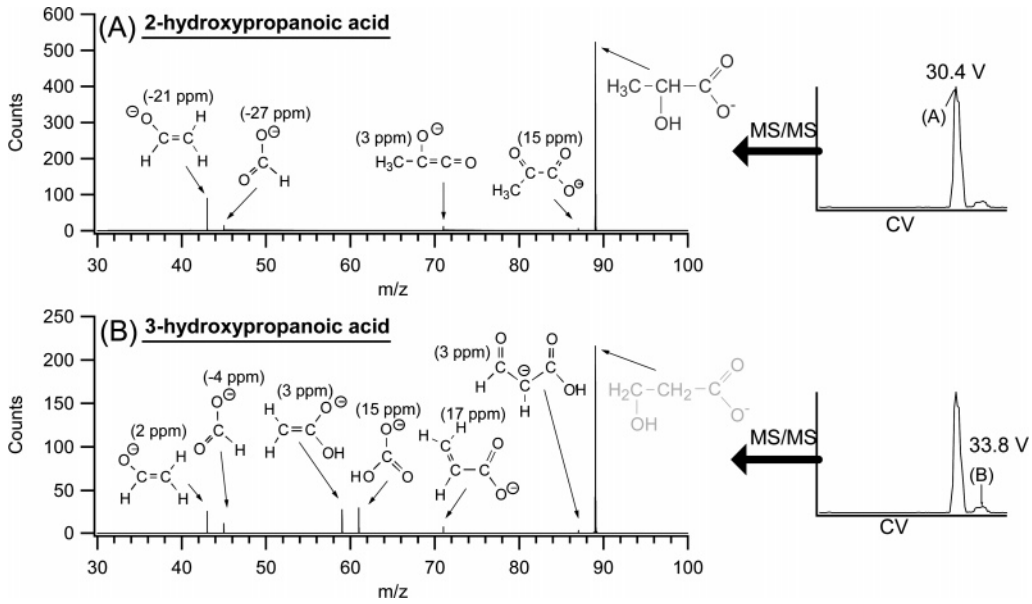

Figure 4. Structural identification of *m*/*z* 89 contaminants of drinking water in tandem mass spectrometry by ESI-FAIMS−MS. MS/MS spectrum of (A) *m*/*z* 89 ion detected at CV 30.4 V at collision energy of 15 eV (100 scans) and (B) *m*/*z* 89 ion detected at CV 33.8 V at collision energy of 15 eV (200 scans).

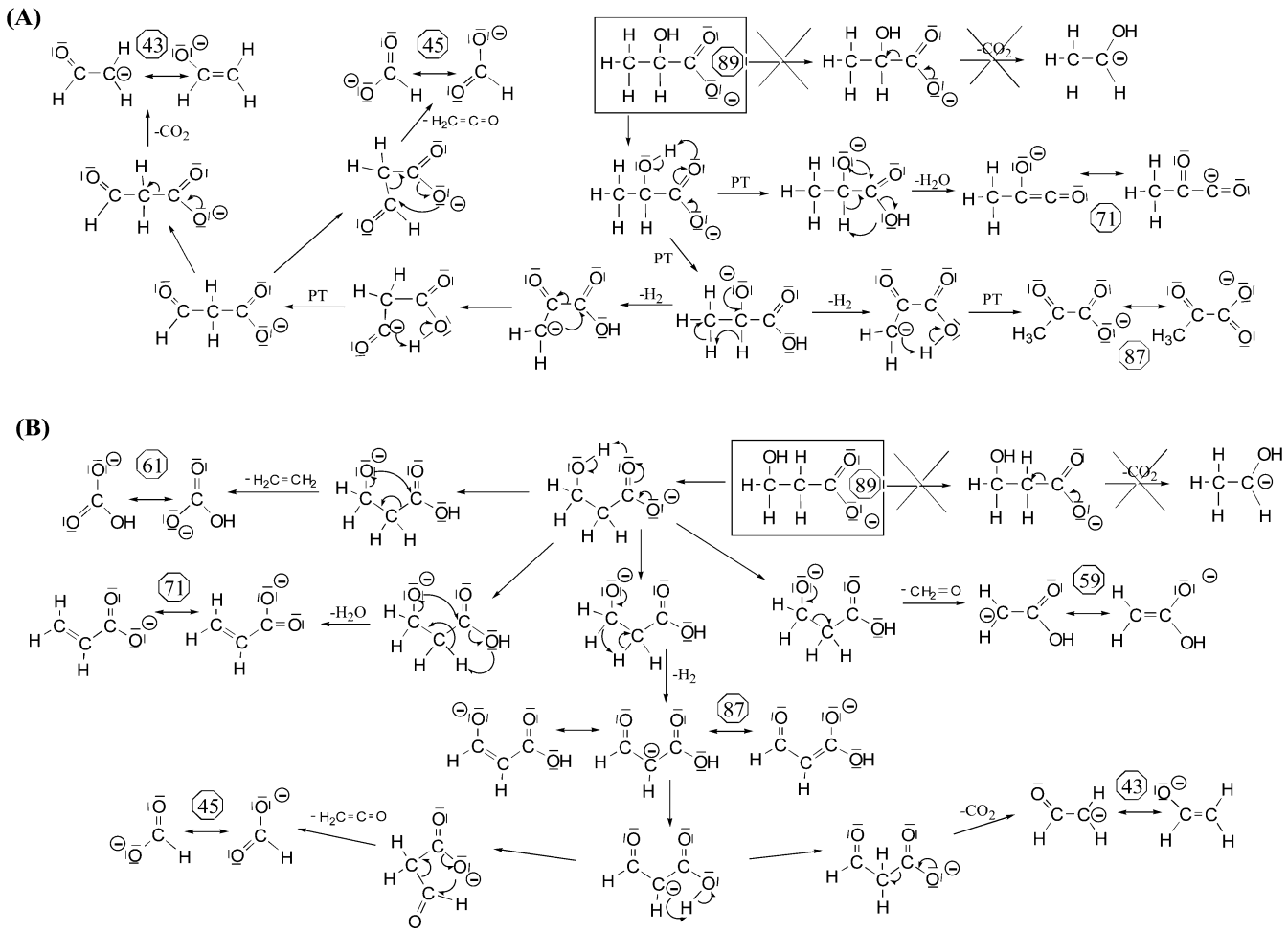

Figure 5. Dissociation patterns of *m*/*z* 89 isomers detected at CV 30.4 V and CV 33.8 V. (A) 2-Hydroxypropanoate detected at CV 30.4 V and (B) 3-hydroxypropanoate detected at CV 33.8 V.

identified in the study) involves redistribution of charge in a structure of collision-excited ions, which leads to a series of reactions engaging the elimination of neutral molecules, proton transfers, and rearrangements to form stable products. All detected fragments could be represented by resonance-stabilized ion structures. The stability of fragment ions with dislocated charge

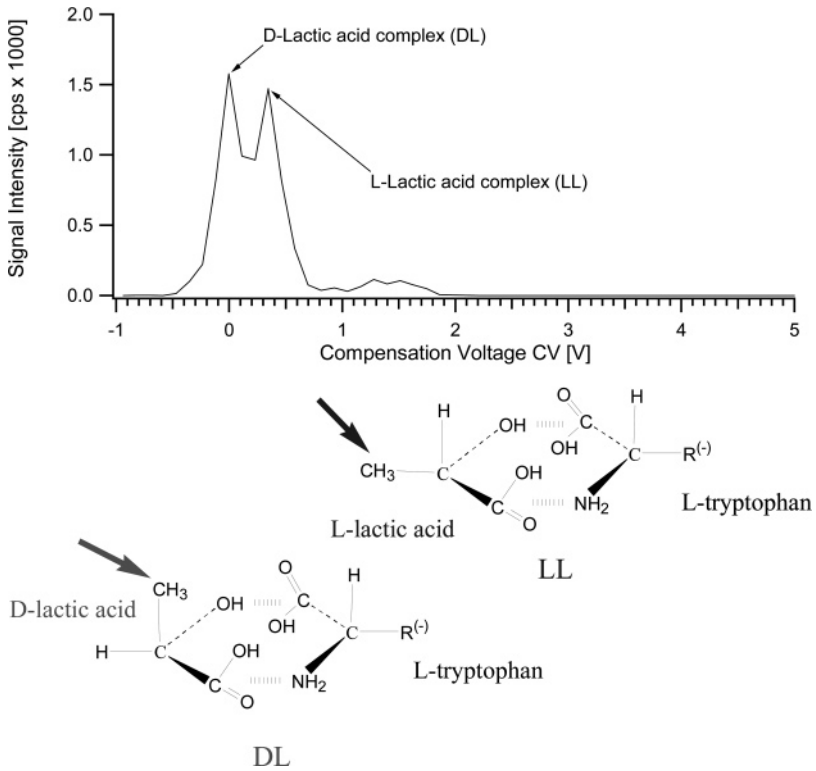

Figure 6. FAIMS separation of D-lactic acid and L-lactic acid as intermolecular complexes of the enantiomers with L-tryptophan. The hypothetical structures of the intermolecular complexes are presented at the bottom of the figure.

is a key factor for their formation and observation in MS/MS. A lack of particular fragments (e.g., the unstable product of elimination of CO_2 from hydroxycarboxylates) is equally important in structural elucidation.

The $C_3H_5O_3^-$ ion observed in the SICV at the CV −5.4 V (Figure 3B) was also investigated in MS/MS. The elemental composition of fragment ions (m/z 87, 71, 61, 59, 45, and 43) of the $C_3H_5O_3^-$ ion at the CV −5.4 V was characteristic of 3-hydroxypropanoate. However, there are two problems related to this structural assignment. First, MS/MS data for the $C_3H_5O_3^-$ ion observed at the CV −5.4 V (Figure 3B) do not exclude the presence of 2-hydroxypropanoate as a result of mass overlaps of the diagnostic fragment ions of these two structural isomers. Second, 3-hydroxypropanoate is transmitted through FAIMS at the CV 33.8 V; thus, it should not be detected at the CV −5.4 V. A careful examination of ions of NOM at the CV −5.4 V (Figure 2 B) showed that the $C_3H_5O_3^-$ ion, detected at the CV −5.4 V, is a product of source fragmentation. The spectral intensity of the $C_3H_5O_3^-$ ion at the CV −5.4 V increased with an increase of kinetic energy of ions entering the mass spectrometer, which suggests that the NOM ions remain intact during FAIMS separation but dissociate in the source (Figure 1) of the mass spectrometer. The complete identification of the $C_3H_5O_3^-$ fragment at the CV −5.4 V could not be accomplished because source fragmentation, in addition to 3-hydroxypropanoate, could potentially produce other structural isomers with the same elemental composition (e.g., 2-hydroxypropanoate). The problem does not exist when the investigated structural isomers are separated by FAIMS. This is a good illustration of the purpose of FAIMS separation in structural identification of isomers. The process of structural identification relies on interpretation of tandem mass spectrometry data to establish a link between observed fragmentation and chemical structure of investigated species. Once the process was completed, we used the chemical standard of 2-hydroxypropanoic acid to confirm our identification procedure. 2-Hydroxypropanoate from the standard was separated at the identical CV (CV 30.4 V) and generated the identical dissociation products as the compound detected in drinking water. The chemical standard of 3-hydroxypropanoic acid is not commercially available.

2-Hydroxypropanoic acid (lactic acid) detected at the CV 30.4 V is chiral and may exist in water in two enantiomeric forms as D-lactic and L-lactic acid. Although enantiomers undergo the same chemical and physical processes in the aquatic environment, differentiation of enantiomers of pollutants is important because their biological properties could vary as a result their enantioselective interactions with other chiral molecules in living organisms. FAIMS separation is normally insensitive to chirality difference. The operation of ESI-FAIMS−MS at the dispersion voltage of −2500 V with the buffer gas containing 70% CO_2 and 30% N_2 provides a unique feature of in situ formation, separation, and detection of gas-phase complexes of carboxylic acids. At such conditions, D-lactic acid and L-lactic acid form with L-tryptophan intermolecular complexes, which are structurally distinctive enough to be separated by FAIMS and stable enough to be introduced into and detected by Q-TOF-MS. The CV spectrum in Figure 6 illustrates FAIMS separation of negatively charged complexes (dimers) of L-lactic acid from the drinking water sample bound to L-tryptophan as well as D-lactic acid from the drinking water sample bound to L-tryptophan. The hypothetical structures of LL and DL complexes are shown in Figure 6. The negative charge is assumed to be retained on the tryptophan side-chain group whereas the polar groups are involved in hydrogen bonding,

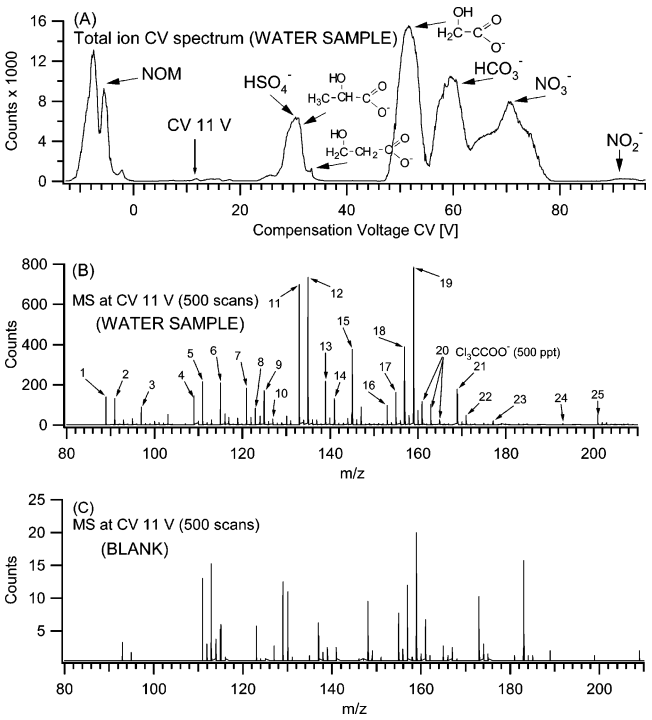

Figure 7. Trace contaminants of drinking water detected at CV 11 V. (A) TICV spectrum of water sample, (B) mass spectrum at water sample at CV 11 V (500 scans), and (C) mass spectrum of blank at CV 11.0 V (500 scans).

which provides a rotational rigidity of the complex ions. A spatial orientation of the methyl group of lactic acid enantiomers is the only structural feature responsible for FAIMS separation of LL and DL dimers. The LL complex with the horizontal methyl group represents a more elongated (linear) structure, which will be transmitted in FAIMS at a slightly larger CV than the DL complex ion with the vertical methyl group. The formation of LL and DL complex ions was accomplished by spiking the water sample containing lactic acid at a low ppm level with L-tryptophan at the concentration of 100 ppm to provide an excess of L-tryptophan. The developed method provided, in a matter of seconds, the determination of the relative abundance of enantiomers of lactic acid in the drinking water. The CV spectrum in Figure 6 indicates that D-lactic acid and L-lactic acid are present in the water sample at approximately the same concentration.

Our identification method, applied to abundant contaminants of drinking water at a ppm concentration level, has shown to be extremely useful for the structural characterization of ultratrace pollutants. Figure 7 A shows the TICV spectrum in which the major components of drinking water contribute to the total ion current observed for the sample. The mass spectrum acquired at the CV 11 V (Figure 7B), at which the total intensity of detected ions is relatively small, contains a number of negatively charged ions representing ultratrace contaminants of drinking water. Among all ions observed in the spectrum, TCA with its isotopic peaks at m/z 161, 163, and 165 (labeled **20**) was the only ion that could be easily identified based on the information from previous studies[16] where TCA was transmitted through FAIMS at the same CV. The standard addition quantification method[16] was used to determine the total concentration of TCA in the analyzed sample at 0.5 part-per-billion (ppb). It gives a rough estimation of concentrations (low and sub ppb) of other compounds detected in water at the CV 11 V. The ion peaks (labeled in the mass spectrum in Figure 7B with numbers from **1** to **25**) with different masses and signal intensities were selected for identification.

An important requirement in chemical analysis at ultratrace level is to determine whether the signals observed for detected species come directly from the sample or are caused by background compounds from solvents and reagents or a detection method itself. The sample preparation in ESI-FAIMS−MS involves only the dilution of a water sample ("preserved" with ammonium chloride) with methanol. Consequently, impurities from methanol and ammonium chloride could potentially contribute to the blank. The mass spectrum in Figure 7C illustrates the determination of the method blank for the species detected at the CV 11 V. The blank mass spectrum was acquired for methanol containing the same concentration of ammonium chloride as the concentration of ammonium chloride in the methanol-diluted water sample. All experimental conditions, instrument settings, and spectrum acquisition parameters used to obtain the blank mass spectrum in Figure 7C were identical to those used to obtain the mass spectrum of the methanol-diluted water sample in Figure 7B. Examination of the intensity of background ions at the CV 11 V in the blank (Figure 7C) with respect to the intensity of ions detected at the CV 11 V in drinking water (Figure 7B) demonstrates clearly that the ESI-FAIMS−MS introduces a very low level of blank. Ion signals of all ultratrace level species selected for structural identification are at least 10 times higher than ion signals of corresponding background ions. It means that the species detected in the mass spectrum in Figure 7B are "real" constituents of drinking water.

Table 2 contains mass spectrometry and tandem mass spectrometry data acquired for the identification of ions detected at the CV 11 V. The measured masses of the investigated ions (Table 2, column 2) have been used to find their best and logical elemental compositions (Table 2, column 5) based on the minimal difference (Table 2, column 4) between the measured mass (Table 2, column 2) and the mass of the postulated elemental composition (Table 2, column 3). The accuracy of mass measurement was determined for three isotopic ions of TCA with known elemental composition. The mass accuracy, expressed as the difference between the measured and theoretical mass and related to the theoretical mass in ppm, obtained for isotopic ions labeled as **20**, **20′**, and **20″** was 16, 15, and 16 ppm, respectively. A similar accuracy of mass measurement, which is sufficient to determine elemental compositions of examined ions, could be expected for all ions listed in Table 2. Table 2 provides also elemental compositions of dissociation (CID) products (Table 2, column 6) determined by mass measurements in tandem mass spectrometry of the investigated ions. The elemental composition of fragment ions, revealing processes of elimination of small molecules from precursor ions, can further confirm the elemental identity of the investigated ions, but it was more important for structural elucidation of ions detected at the CV 11 V.

Figure 8 shows MS/MS spectra of five CV 11 V ions as well as their structures and structures of their dissociation products, which have been established based on fragmentation patterns illustrated in Figure 9. The dissociation reactions in Figure 9

Table 2. Determination of Elemental Compositions of Ions Representing Ultratrace Contaminants of Drinking Water Detected at the CV 11 V

ion	measd m_M	calcd m_C	$(m_M - m_{C1thr})/m_C \times 10^6$ (ppm)	elemental composition	CID products
1	88.9798	88.9797	−2	$C_3H_2O^{35}Cl$	
2	90.9767	90.9770	−3	$C_3H_2O^{37}Cl$	
3	96.9930	96.9931	−1	C_4HO_3	
4	108.9710	108.9697	11	$C_2H_2O_3{}^{35}Cl$	$C_2O_2{}^{35}Cl$
5	111.0090	111.0082	2	$C_5H_3O_3$	
6	115.0040	115.0036	3	$C_4H_3O_4$	$C_3H_3O_2$
7	120.9720	120.9697	18	$C_3H_2O_3{}^{35}Cl$	CHO_2, $C_2H_2O^{35}Cl$
8	122.9680	122.9668	10	$C_3H_2O_3{}^{37}Cl$	CHO_2, $C_2H_2O^{37}Cl$
9	124.9550	124.9566	−13	$C_3H_3O^{35}Cl_2$	
10	126.9546	126.9537	7	$C_3H_3O^{35}Cl^{37}Cl$	
11	132.9706	132.9697	6	$C_4H_2O_3{}^{35}Cl$	$C_3H_2O^{35}Cl$
12	134.9679	134.9668	8	$C_4H_2O_3{}^{37}Cl$	$C_3H_2O^{37}Cl$
13	138.9369	138.9359	7	$C_3HO_2{}^{35}Cl_2$	
14	140.9845	140.9829	11	C_5HO_5	C_4HO_3
15	145.0520	145.0506	9	$C_6H_9O_4$	C_5H_7O, $C_5H_9O_3$, $C_5H_7O_3$, $C_6H_7O_3$
16	152.9613	152.9596	11	$C_3H_2O_5{}^{35}Cl$	$C_2O_2{}^{35}Cl$, $C_2H_2O_3{}^{35}Cl$
17	155.0000	154.9985	9	$C_6H_3O_5$	$C_5H_3O_3$
18	156.9470	156.9464	3	$C_3H_3O_3{}^{35}Cl_2$	$C_2H_3O_2$, CHO_3, $C_3HO_2{}^{35}Cl_2$
19	158.9950	158.9935	9	$C_5H_3O_6$	$C_3H_3O_2$, $C_4H_3O_4$
20	160.8995	160.8969	16	$C_2O_2{}^{35}Cl_3$	$C^{35}Cl_3$
20′	162.8964	162.8940	15	$C_2O_2{}^{35}Cl_2{}^{37}Cl$	$C^{35}Cl_2{}^{37}Cl$
20″	164.8937	164.8911	16	$C_2O_2{}^{35}Cl^{37}Cl_2$	$C^{35}Cl^{37}Cl_2$
21	168.9456	168.9464	−5	$C_4H_3O_3{}^{35}Cl_2$	$C_2H_3O_2$, $C_3H_3O^{35}Cl_2$
22	170.9440	170.9435	3	$C_4H_3O_3{}^{35}Cl^{37}Cl$	$C_2H_3O_2$, $C_3H_3O^{35}Cl^{37}Cl$
23	170.0010	177.0040	−17	$C_5H_5O_7$	
24	192.9960	192.9989	−15	$C_5H_5O_8$	$C_4H_5O_6$
25	200.9400	200.9363	18	$C_4H_3O_5{}^{35}Cl_2$	$C_3HO_2{}^{35}Cl_2$, $C_3HO_3{}^{35}Cl_2$, $C_3H_3O_3{}^{35}Cl_2$

represent fragmentation pathways of other investigated ions, and they will support the following discussion on elucidation of chemical structures (Figure 10) of ions detected at the CV 11 V. Figure 8E shows the MS/MS spectrum of the ion labeled **25** with the elemental composition of $C_4H_3O_5{}^{35}Cl_2$. The elemental compositions of fragment ions were determined by mass measurements (accuracy of mass measurement is given for all fragment ions in Figure 8). The structure of **25** was established based on its fragmentation reactions (Figure 8E). The ion **25** (m/z 201 in Figure 8E) dissociates to produce the m/z 157 ion by elimination of CO_2 from its structure. The formation of the resonance-stabilized m/z 157 ion (decarboxylation product) is facilitated by the presence of the second α-carboxylic group in the structure of the precursor ion. The elimination of CO_2 from **25,** followed by PT, leads to formation of the m/z 157 ion, which generates the m/z 155 ion and the 139 m/z ion by loss of H_2 and H_2O, respectively. The last two dissociation patterns are similar to those of α-hydroxycarboxylate (Figure 5A) with a difference that the products of rearrangement, proton transfer, and dissociation of the m/z 155 ion are not observed as a result of delocalization of negative charge at the terminal carbon. The charge delocalization is provided by inductive effect of chlorine atoms substituted at the terminal carbon. The lack of dissociation products at m/z 61 and m/z 93, which would be diagnostic for the dissociation of β-hydroxycarboxylate (Figure 5B), is also important to establish the (α) position of the OH group in the structure. In summary, the dissociation patterns of **25** imply the presence of two carboxylic groups (in α position one to each other) and one hydroxyl group in α position. This information is sufficient to determine the chemical structure of **25**. The ion **24** dissociates by the elimination of CO_2. The only chemical structure that would be consistent with the elemental composition and the fragmentation of **24** is the dicarboxylic acid shown in Figure 10. A sequential elimination of CO_2 from **24** is not feasible. The elimination of the CO_2 group at the carbon linked to the carbonyl group is facilitated by formation of the carboanion with negative charge delocalized on the carbonyl group. The elimination of the CO_2 group at the carbon linked to two hydroxyl group does not take place because it would involve the formation of unstable ion with localized charge. The same CID behavior was observed for the decarboxylation reactions of α- and β-hydroxypropanoates (Figure 5A and Figure 5B). It is important to note that two structural isomers of **24** would generate CID products different from **24**. The isomer with the carboxyl and the hydroxyl group in α position would, analogically to **25**, eliminate CO_2 followed by loss of H_2O. The isomer with the carboxyl and the carbonyl group in α position would eliminate CO_2 followed by loss of another CO_2 or eliminate CO_2 followed by loss of H_2O. The ion **23** did not fragment, and its chemical structure shown in Figure 10 is the only structure that satisfies this experimental observation. The MS/MS spectrum of **21** is shown in Figure 8D. The dissociation reactions of **21** are illustrated in Figure 9D, in which two fragment ions of **21** at m/z 125 and 59 are formed by elimination of CO_2 and dichloroketene, respectively. The presence of the m/z 45 fragment ion in the MS/MS spectrum of **21** indicates that another structural isomer of **21** is transmitted by FAIMS at the CV 11 V. The

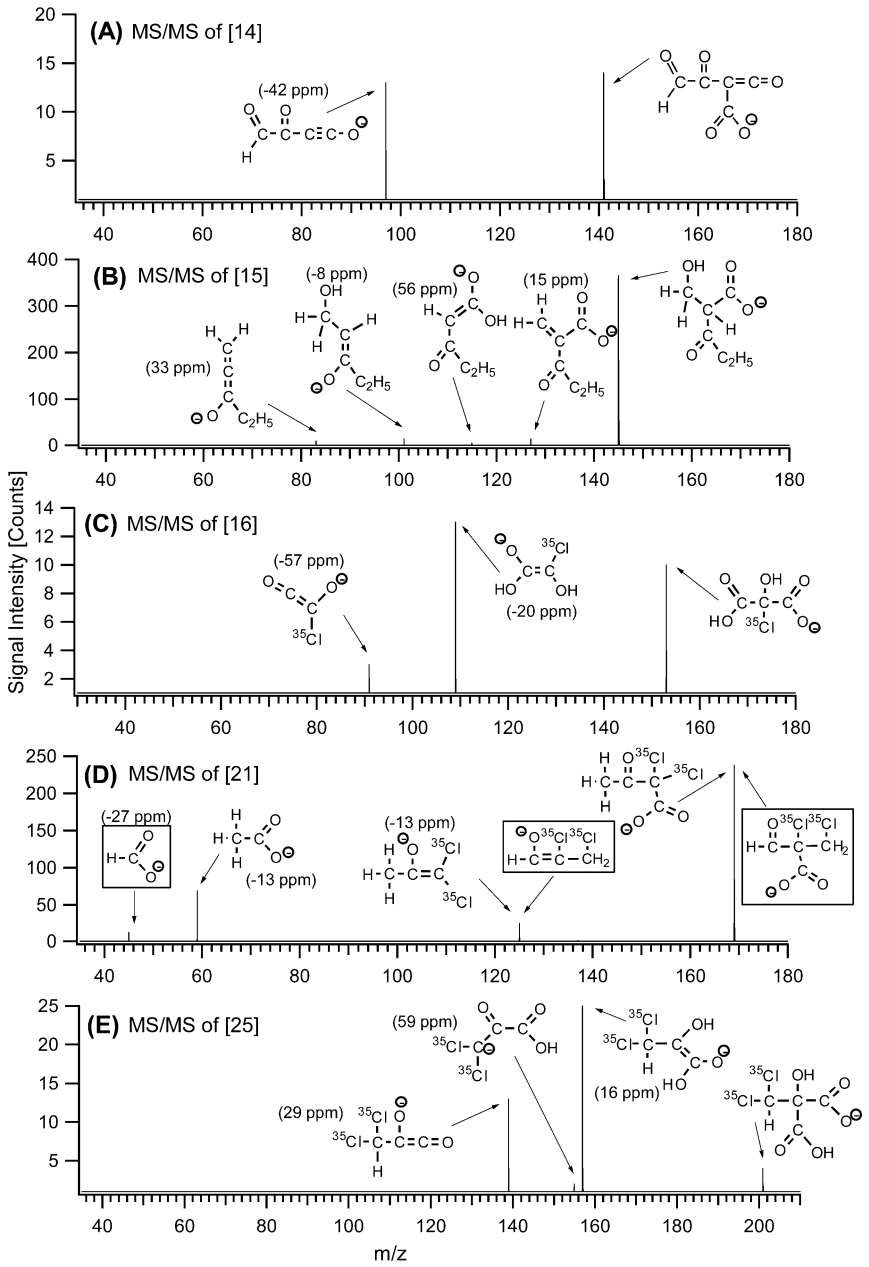

Figure 8. Structural identification of trace contaminants of drinking water, detected at CV 11 V, in tandem mass spectrometry. MS/MS spectrum of (A) **14** at collision energy of 3.4 eV (500 scans), (B) **15** at collision energy of 5.0 eV (500 scans), (C) **16** at collision energy of 3.6 eV (500 scans), (D) **21** at collision energy of 5.2 eV (500 scans), and (E) **25** at collision energy of 3.8 eV (500 scans).

structures of the minor structural isomer of **21** and its dissociation products are presented in the boxes in Figure 8D. The ion **22** has the same structure as **21** but contains one ^{37}Cl isotope. The identity of **20**, **20′**, and **20″** was confirmed by the detection of their dissociation products generated by elimination of CO_2 from TCA. The formation of decarboxylation products of TCA is facilitated by the inductive effect of three chlorine atoms located at α-carbon. The unique elemental composition of **19** and its fragmentation by consecutive elimination of CO_2 were key factors to establish its chemical structure. The elimination of H_2O and Cl_2CO as well as the formation of the m/z 61 with the elemental composition of CHO_3 from **18** represents characteristic fragmentation patterns of β-hydroxypropanoate (Figure 5B) containing two chlorine atoms at β-carbon. The chemical structure of **17** is similar to the structures established for **14**, **12**, and **11**. All these ions are fragile and easily fragment in MS/MS by elimination of CO_2. The MS/MS spectrum of **14** is shown in Figure 8A. The dissociation patterns of **14**, illustrated in Figure 9A, can serve as a reference for the structurally similar ions of **17**, **12**, and **11**. The m/z 141 ion **14**, represented by two structures (closed and open), dissociates by elimination of CO_2 to form the stable m/z 97 fragment. The same fragmentation pattern is observed for **17**, **12**, and **11**. We believe that **17**, **14**, **12**, and **11** do not originate from a water sample but they represent products of source fragmentation of α-dicarboxylic acid. The structure of an anion of the α-dicarboxylic acid, which would form **14** by elimination of H_2O, is shown in Figure 9A. The precursor ions of **11**, **12**, **14**, and **17** have not been observed in the spectrum at the CV 11 V. It may suggest that anions of α-dicarboxylic acids with hydrogen at α position are extremely fragile species prone to

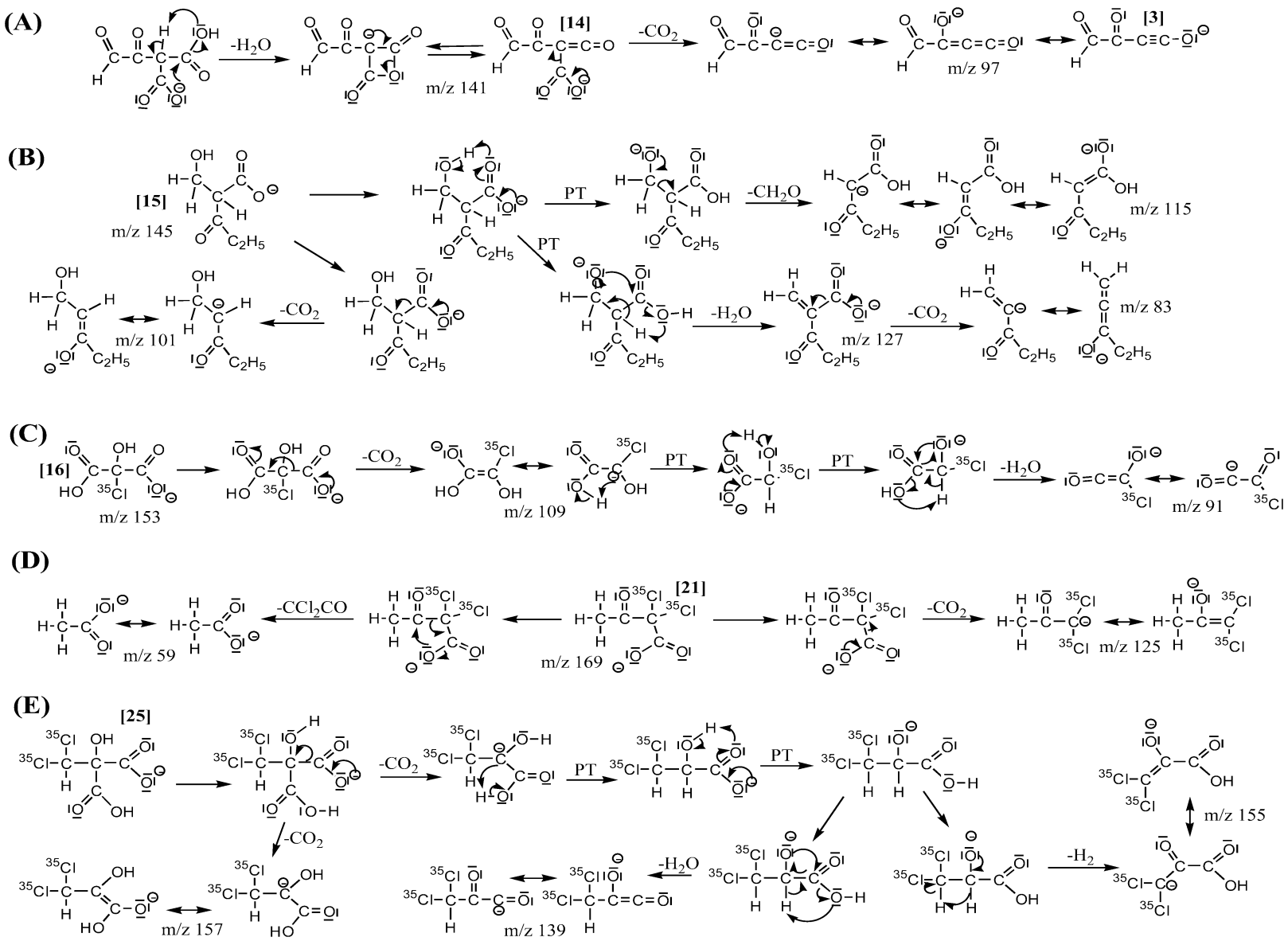

Figure 9. Fragmentation patterns of ions of trace contaminants of drinking water detected at CV 11 V. Dissociation reactions of (A) **14**, (B) **15**, (C) **16**, (D) **21**, and (E) **25**.

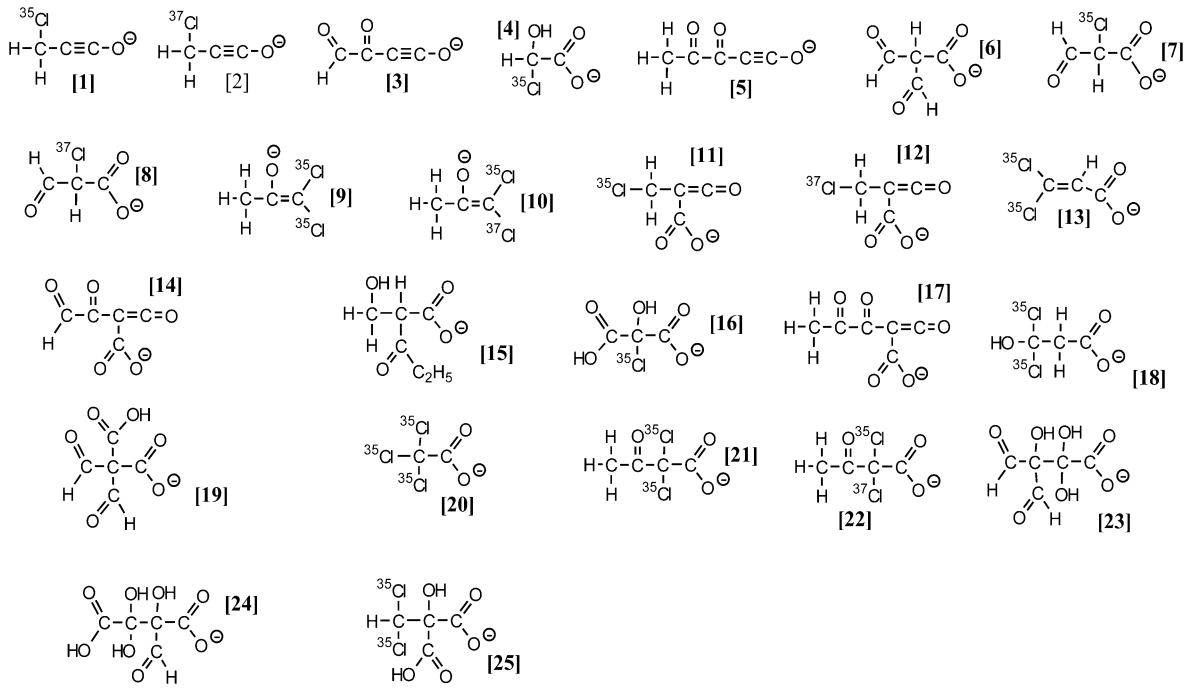

Figure 10. Chemical structures of contaminants of drinking water detected at CV 11 V.

source fragmentation by loss of H_2O. The identification of **16** was based on the MS/MS spectrum of **16** (Figure 8C) and its dissociation patterns (Figure 8C) showing elimination of CO_2 with subsequent elimination of H_2O following proton transfers. The detection of four fragmentation products of **15** (Figure 8B), which originated from **15** in CID processes (Figure 9B) of elimination of CO_2, elimination of H_2CO, elimination of H_2O, and elimination of H_2O followed by loss of CO_2, provided essential information for structural elucidation of **15**. The ions **13**, **10**, and **9** have not generated fragments in MS/MS. Consequently, it was not possible to establish exact positions of chlorine and hydrogen atoms in the structures of **13**, **10**, and **9** shown in Figure 10. Based on additional experiments where the detection was carried out at different kinetic energies of ions at the entrance of the mass spectrometer, we determined that **13**, **10**, and **9** are products of source fragmentation of larger ions transmitted at the CV 11 V. The ions **13, 10**, and **9** could originate from **18**, **22**, and **21**, respectively. The postulated chemical structures of **13, 10**, and **9** (Figure 10) are based on this assumption. The structures of ions **7** and **8** reflect their fragmentation patterns (elimination of CO_2 and formation of formic acid) similar to those presented for **21**. The elucidation of chemical structures of **1**−**6** was accomplished based on their unique elemental compositions and information from tandem mass spectrometry. The dissociation of **6** and **4** by the elimination of CO_2 and H_2O, respectively, as well as no fragmentation observed for **5**, **3**, **2**, and **1** were critical pieces of information for structural assignment of **1**−**6**. The identified species **6**, **5**, **4**, **3**, **2**, and **1** do not represent water contaminants, but they are products of source fragmentation of **19**, **17**, **16**, **14**, **12**, and **11**, respectively. The chemical structures of all investigated ions are presented in Figure 10.

Carboxylic acids at the CV 11 V represent a group of disinfection byproducts that has not been identified in drinking water before. Their chemical structures, with the exception of fragment ions, are similar to the structure of TCA (**19**) in the way that the carboxylic acids are substituted at α position by several bulky groups. This structural similarity could explain their detection at the same CV. The identification of chlorinated carboxylic acids showed that a relative intensity of ion peaks containing ^{35}Cl and ^{37}Cl isotopes, determined at a particular CV, is different from the relative intensity commonly observed in mass spectrometry. FAIMS can separate isotopic ions, which was observed in Figure 7B for the m/z 133 $C_4H_2O_3{}^{35}Cl$ (**11**) and the m/z 135 $C_4H_2O_3{}^{37}Cl$ (**12**). The optimal transmission of **11** in FAIMS occurs at a lower CV than the optimal transmission of **12**, and the relative intensity of **11** and **12** at the CV 11 V cannot be used for the identification of species containing chlorine isotopes. This small disadvantage of ESI-FAIMS−MS, however, is greatly compensated by several advantages of the method demonstrated for the identification of highly polar contaminants in drinking water.

The paper focuses on the structural identification of randomly selected, nontarget contaminants detected in drinking water. The most intriguing contaminant identified in the study, however, was the most abundant polar component of the sample. The largest CV peak, observed in the TICV spectrum at the CV 51 V in Figure 7A, corresponds to the anion of glycolic acid ($CH_2OHCOOH$). The identification of glycolate was accomplished by the determination of its elemental composition and examination of its dissociation patterns (elimination of H_2O, elimination of H_2, and elimination of H_2 followed by elimination of CO) similar to those of α-hydroxycarboxylate (Figure 5A). The identification of glycolic acid was confirmed by using the chemical standard. It is surprising that the most abundant organic component of drinking water detected by the method has never been considered as a water pollutant. Glycolic acid cannot be found on the EPA drinking water

contaminant list or drinking water contaminant candidate list, despite the fact that it is present in drinking water at a high ppm concentration level. Glycolic acid, in laboratory rats which metabolize and eliminate glycolic acid faster than humans, was found to be toxic to kidneys, moreover, the ingestion of glycolic acid, on a daily basis, was associated with a moderate maternal toxicity.[22,23] We are currently conducting quantitative studies of glycolic acid in drinking water that show ubiquitous nature of this new disinfection byproduct discovered by ESI-FAIMS−MS.

CONCLUSIONS

The intention of the authors was to demonstrate the analytical potential of the ESI-FAIMS−MS method in the analysis of highly polar contaminants in drinking water. The structural identification of a relatively small group of contaminants could not be so easily accomplished by any other analytical method available today. The continuous mode of FAIMS separation (no time limit for the availability of ions for MS and MS/MS experiments) was the key element to obtain high-quality spectral information, so critical for structural elucidation of nontarget analytes. The gas-phase separation process in FAIMS seems to be very effective in eliminating background interferences and providing remarkable selectivity, which is reflected in the MS and MS/MS spectra of compounds analyzed at sub-ppb concentrations. Finally, the FAIMS−MS interface allows for detection of very fragile ions. The combination of these features and the feasibility of analyzing water samples directly without sample preparation offer new opportunities in water analysis of highly polar compounds. The high screening capacity of the technique could be used in monitoring a large population of previously identified water pollutants. De novo identification method, presented here for drinking water, could also be applied to other complex mixtures with a purpose of chemical characterization of sample's components.

(22) Richardson, D. E. *Toxicol. Appl. Pharm.* **1965**, *7*, 507.
(23) Munley, S. M. *Drug Chem. Toxicol.* **1999**, *22* (4), 569.

ACKNOWLEDGMENT

The authors thank National Sciences and Research Council of Canada (NSERC) and Canada Foundation for Innovation (CFI) for their support.

Received for review March 1, 2006. Accepted March 29, 2006.

AC060384X